

# Detection of a Supervoid Aligned with the Cold Spot of the Cosmic Microwave Background

István Szapudi<sup>1</sup>, András Kovács<sup>2,3</sup>, Benjamin R. Granett<sup>4</sup>, Zsolt Frei<sup>2,3</sup>, Joseph Silk<sup>5</sup>, Will Burgett<sup>1</sup>, Shaun Cole<sup>6</sup>, Peter W. Draper<sup>6</sup>, Daniel J. Farrow<sup>6</sup>, Nicholas Kaiser<sup>1</sup>, Eugene A. Magnier<sup>1</sup>, Nigel Metcalfe<sup>6</sup>, Jeffrey S. Morgan<sup>1</sup>, Paul Price<sup>7</sup>, John Tonry<sup>1</sup>, Richard Wainscoat<sup>1</sup>

<sup>1</sup> *Institute for Astronomy, University of Hawaii 2680 Woodlawn Drive, Honolulu, HI, 96822, USA*

<sup>2</sup> *Institute of Physics, Eötvös Loránd University, 1117 Pázmány Péter sétány 1/A Budapest, Hungary*

<sup>3</sup> *MTA-ELTE EIRSA “Lendület” Astrophysics Research Group, 1117 Pázmány Péter sétány 1/A Budapest, Hungary*

<sup>4</sup> *INAF OA Brera, Via E. Bianchi 46, Merate, Italy*

<sup>5</sup> *Department of Physics and Astronomy, The Johns Hopkins University, Baltimore MD 21218, USA*

<sup>6</sup> *Department of Physics, Durham University, South Road, Durham DH1 3LE, UK*

<sup>7</sup> *Department of Astrophysical Sciences, Princeton University, Princeton, NJ 08544*

Submitted 2014

## ABSTRACT

We use the WISE-2MASS infrared galaxy catalog matched with Pan-STARRS1 (PS1) galaxies to search for a supervoid in the direction of the Cosmic Microwave Background Cold Spot. Our imaging catalog has median redshift  $z \simeq 0.14$ , and we obtain photometric redshifts from PS1 optical colours to create a tomographic map of the galaxy distribution. The radial profile centred on the Cold Spot shows a large low density region, extending over 10’s of degrees. Motivated by previous Cosmic Microwave Background results, we test for underdensities within two angular radii,  $5^\circ$ , and  $15^\circ$ . The counts in photometric redshift bins show significantly low densities at high significance,  $\gtrsim 5\sigma$  and  $\gtrsim 6\sigma$ , respectively, for the two fiducial radii. The line-of-sight position of the deepest region of the void is  $z \simeq 0.15 - 0.25$ . Our data, combined with an earlier measurement by Granett et al. (2010), are consistent with a large  $R_{\text{void}} = (192 \pm 15)h^{-1}\text{Mpc}$  ( $2\sigma$ ) supervoid with  $\delta \simeq -0.13 \pm 0.03$  centered at  $z = 0.22 \pm 0.01$ . Such a supervoid, constituting a  $\simeq 3.5 - 5\sigma$  fluctuation in a Gaussian distribution of the  $\Lambda\text{CDM}$  model, is a plausible cause for the Cold Spot.

**Key words:** surveys – cosmology: observations – large-scale structure of Universe – cosmic background radiation

## 1 INTRODUCTION

The Cold Spot (CS) of the Cosmic Microwave Background (CMB) is an exceptionally cold  $-70\mu\text{K}$  area centred on  $(l, b) \simeq (209^\circ, -57^\circ)$  Galactic coordinates. It was first detected in the Wilkinson Microwave Anisotropy Probe (Bennett et al. 2012) maps at  $\simeq 3\sigma$  significance using wavelet filtering (Vielva et al. 2004; Cruz et al. 2005). The CS is perhaps the most significant among the “anomalies”, potential departures from isotropic and/or Gaussian statistics, and all confirmed by *Planck* (Planck 2013 results. XXIII. 2013). Explanations of the CS range from statistical fluke through hitherto undiscovered physics, e.g., textures (Cruz et al. 2008; Vielva 2010), to the linear and nonlinear ISW effect (Sachs & Wolfe 1967; Rees & Sciama 1968) from a  $\gtrsim 200h^{-1}\text{Mpc}$  supervoid centred on the CS (Inoue & Silk 2006, 2007; Inoue et al. 2010). The latter would be readily detectable in

large scale structure surveys thus motivating several observational studies.

A low density region approximately aligned with the CS was detected in a catalog of radio galaxies (Rudnick et al. 2007), although its significance has been disputed (Smith & Huterer 2010). A targeted redshift survey in the area (Bremer et al. 2010) found no evidence for a void in the redshift range of  $0.35 < z < 1$ , while an imaging survey with photometric redshifts (Granett et al. 2010) excluded the presence of a large underdensity of  $\delta \simeq -0.3$  between redshifts of  $0.5 < z < 0.9$  and finding none at  $0.3 < z < 0.5$ . Both of these surveys ran out of volume at low redshifts due to their small survey area, although the data are consistent with the presence of a void at  $z < 0.3$  with low significance (Granett et al. 2010). In a shallow photometric redshift catalogue constructed from the Two Micron All Sky Survey (Skrutskie et al. 2006, 2MASS) and SuperCOSMOS (Hambly et al. 2001) with a median redshift of  $z = 0.08$  an under-density was found

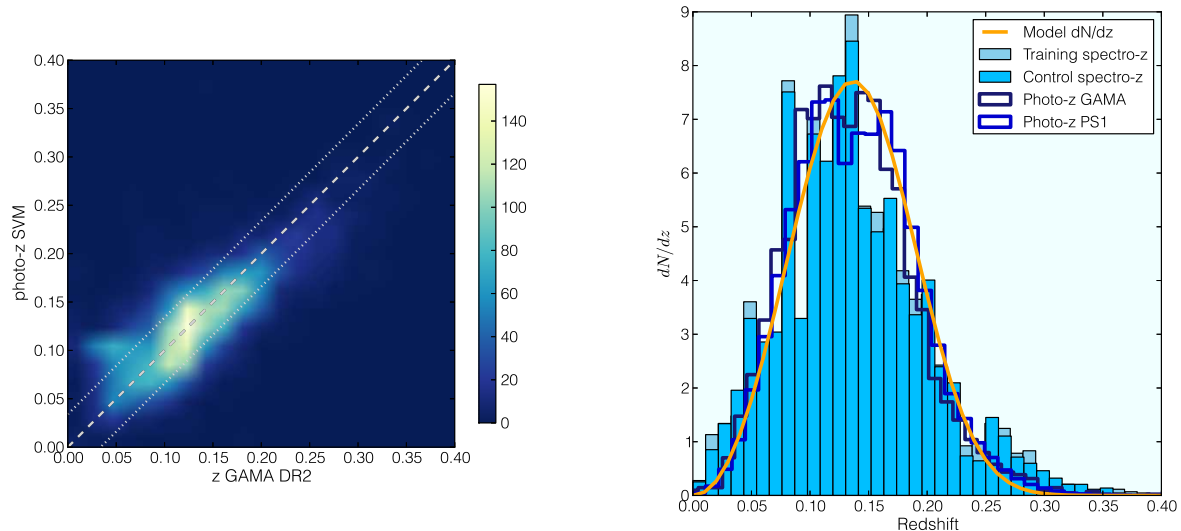


**Figure 1.** The left panel shows the photo- $z$  accuracy achieved by the SVM. Dotted lines indicate the  $\sigma_z \approx 0.034$   $1\sigma$  error bars around the expectation. The right panel illustrates the normalized redshift distributions of our subsamples used in the photo- $z$  pipeline; training and control sets selected in GAMA, photo- $z$  distributions estimated for the WISE-2MASS-PS1-GAMA control sample, and photo- $z$ 's of interest in the WISE-2MASS-PS1 matched area. The median redshift of all subsamples is  $z \simeq 0.14$ .

(Francis & Peacock 2010) that can account for a CMB decrement of  $\Delta T \simeq -7\mu\text{K}$  in the standard  $\Lambda$ -Cold Dark Matter ( $\Lambda\text{CDM}$ ) cosmology. While so far no void was found that could fully explain the CS, there is strong,  $\gtrsim 4.4\sigma$ , statistical evidence that superstructures imprint on the CMB as cold and hot spots (Granett et al. 2008, 2009; Pápai & Szapudi 2010; Planck 2013 results. XXIII. 2013; Cai et al. 2013). Note that the imprinted temperature in all of these studies is significantly colder than simple estimates from linear ISW (e.g., Rudnick et al. 2007; Pápai & Szapudi 2010; Pápai et al. 2011) would suggest.

The Wide-field Infrared Survey Explorer (Wright et al. 2010, WISE) all-sky survey effectively probes low redshift  $z \leq 0.3$  unconstrained by previous studies. Using the WISE-2MASS all sky galaxy map of Kovács & Szapudi (2014) as a base catalog, we match a  $1,300 \square^\circ$  area with the PV1.2 reprocessing of Pan-STARRS1 (hereafter PS1, Kaiser 2004), adding optical colours for each objects. In the resulting catalog with photometric redshifts we test for the presence of a large low density region, a supervoid, centered on the CS.

We defined the centre of the CS from the latest *Planck* results (Planck 2013 results. XXIV. 2013). Based on the literature, we decided in advance to test for an underdensity at  $5^\circ$  (Vielva et al. 2004; Cruz et al. 2005; Rudnick et al. 2007; Granett et al. 2010; Bremer et al. 2010) and  $15^\circ$  (Zhang & Huterer 2010; Inoue et al. 2010) of radii. The fact that these values gleaned from CMB independently of our (large scale structure) data simplifies the interpretation of our results in the Bayesian framework, in particular, minimize any posteriori bias.

The paper is organised as follows. Data sets and map making algorithms are described in Section 2; our observational results are presented in Section 3; the final section contains a summary, discussion and interpretation of our results.

## 2 DATASETS AND METHODOLOGY

Initially, we select galaxies from the WISE-2MASS catalog (Kovács & Szapudi 2014) containing sources to flux limits of  $W1_{\text{WISE}} \leq 15.2$  mag and  $W1_{\text{WISE}} - J_{2\text{MASS}} \leq -1.7$ . We add a further limit of  $J_{2\text{MASS}} \leq 16.5$  mag to ensure spatial homogeneity based on our experiments. This refinement shifts the median redshift of the sample to  $z \simeq 0.14$ . The catalog covers  $21,200 \square^\circ$  after masking. We mask pixels with  $E(B - V) \geq 0.1$ , and regions at galactic latitudes  $|b| < 20^\circ$  to exclude potentially contaminated regions near the Galactic plane (Schlegel et al. 1998). These conservative limits result in a dataset deeper than 2MASS and more uniform than WISE. These galaxies have been matched with Pan-STARRS1 objects within a  $50^\circ \times 50^\circ$  area centred on the CS, except for a Dec  $\geq -28.0$  cut to conform to the PS1 boundary. We used PV1.2 reprocessing of PS1 in an area of  $1,300 \square^\circ$ .

For matching we applied a nearest neighbour search using the `scipy kd-Tree` algorithm with  $1''$  matching radius, finding a PS1 pair for 86% of the infrared galaxies, and resulting 73,100 objects in the final catalog. Galaxies without a PS1 match are faint in the optical, and predominantly massive early-type galaxies at  $z > 1$  (Yan et al. 2012). For PS1, we required a proper measurement of Kron (Kron 1980) and PSF magnitudes in  $g_{\text{P1}}$ ,  $r_{\text{P1}}$  and  $i_{\text{P1}}$  bands that were used to construct photometric redshifts (photo- $z$ 's) with a Support Vector Machine (SVM) algorithm, and the `python scikit-learn` (Pedregosa et al. 2011) routines in regression mode. The training and control sets were created matching WISE-2MASS, PS1, and the Galaxy and Mass Assembly (GAMA, Driver et al. 2011) redshift survey. We chose a Gaussian kernel for our SVM and trained on 80% of the GAMA redshifts, while the rest were used for a control set. We empirically tuned the standard SVM parameters, finding the best performance when using  $C = 10.0$ , and  $\gamma = 0.1$ . We characterize our photo- $z$  quality with the error  $\sigma_z = \sqrt{\langle (z_{\text{phot}} - z_{\text{spec}})^2 \rangle}$ , finding  $\sigma_z \approx 0.034$ , as summarised in Figure 1.

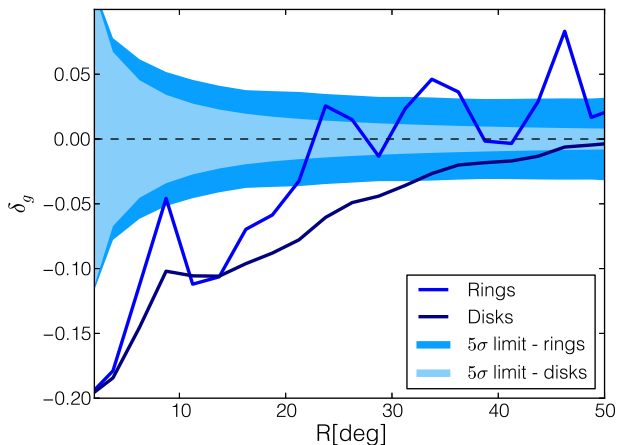


**Figure 2.** Radial galaxy density profile of the WISE-2MASS galaxy catalog, centred on the CS. The under-density is detected out to 10’s of degrees in radius, consistent with an  $r \approx 200h^{-1}\text{Mpc}$  supervoid with  $\delta_g \simeq -0.2$  deepening in its centre. Note that the deeper central region is surrounded by a denser shell.

### 3 RESULTS

#### 3.1 Radial profiles

We first study the Cold Spot region in projection, using the WISE-2MASS galaxies only. We measure radial galaxy density profiles in rings and disks centered on the CS in a bin size of  $2.5^\circ$ , allowing identification of relatively small-scale structures. Error bars represent Poisson fluctuations in our measurement, calculated from the total number of galaxies in a ring or disk. Note that error bars are uncorrelated only for rings. Figure 2 shows a significant depression of sources. At our pre-determined radii,  $5^\circ$  and  $15^\circ$ , we have a signal-to-noise ratio  $S/N \sim 12$  for rings.

The size of the underdensity is surprisingly large: it is detected up to  $\sim 20^\circ$  with high ( $\gtrsim 5\sigma$ ) significance. In addition, the profile has ring-like over density surrounding the CS region at large angular radii. This is consistent with a supervoid surrounded by a gentle compensation that converges to the average galaxy density at  $\sim 50^\circ$  (see e.g., Pápai et al. 2011).

#### 3.2 Counts as a function of photometric redshift

We use the WISE-2MASS-PS1 galaxy catalog with photo- $z$  information to constrain the position, size, and depth of supervoids. We count galaxies as a function of redshift in disks centred on the CS at our fiducial angular radii,  $r = 5^\circ$ , and  $15^\circ$ , and compare the results to the average redshift distribution of our sample. Since the latter disks are cut by the PS1 mask, we compensate for that in our tests. We fit the observed redshift distribution with a model  $dN/dz \propto e^{-(z/z_0)^\alpha} z^\beta$ , estimating the parameters as  $z_0 = 0.16$ ,  $\alpha = 3.1$ , and  $\beta = 1.9$ . The average redshift distribution was obtained by counting all galaxies within our catalog outside the  $15^\circ$  test circle, i.e. using  $750 \square^\circ$ , and errors of this measurement are propagated to our determination of the underdensity.

We created subsamples of galaxies in photo- $z$  bins of width  $\Delta z = 0.035$ , and compared the galaxy counts we measure inside the test circles to that of the control area. We find  $S/N \sim 5$  and  $S/N \sim 6$  for the deepest under-density bins for  $r = 5^\circ$  and  $15^\circ$ .

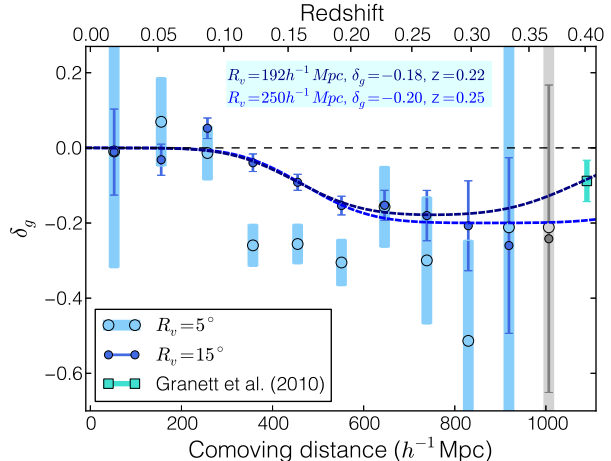


**Figure 3.** Our measurements of the galaxy density in the line-of-sight using the  $\Delta z = 0.035$  photo- $z$  bins we defined. We detected a significant depression in galaxy density in  $r = 5^\circ$  and  $15^\circ$  test circles. We used our simple modeling tool to examine the effects of photo- $z$  errors, and test the consistency of simple top-hat voids with our measurements. The last bin (shown in grey) was excluded from the analysis, and a data point by Granett et al (2010) accounts for the higher redshift part of the measurement. See text for details.

We add a measurement of Granett et al. (2010) in the photo- $z$  bin centered at  $z = 0.4$  in order to extend our analysis to higher redshifts in Fig. 3.

To quantify our results further, we build toy models from top-hat voids in the  $z$  direction to model the smearing by the photo- $z$  errors. The initial top hat with three parameters, redshift ( $z_{\text{void}}$ ), radius ( $R_{\text{void}}$ ), and central depth ( $\delta_g$ ), was smoothed using the distribution corresponding to the photometric redshift errors. The model redshift distribution was then multiplied with this smeared profile.

The void model can be compared to observations using a  $\chi^2$ -based maximum likelihood parameter estimation. We focus on the largest scale underdensity, therefore we only use the  $r = 15^\circ$  data, and replace our last bin with the measurement of Granett et al. (2010)). This gives  $n = 11$  bins with  $k = 3$  parameters, thus the degrees of freedom are  $\nu = n - k = 8$ . We find a  $\chi^2_{15^\circ} = 92.4$  for the null hypothesis of no void. The best fit parameters with marginalized errors are  $z_{\text{void}} = 0.22 \pm 0.01$  ( $2\sigma$ ),  $R_{\text{void}} = (192 \pm 15)h^{-1}\text{Mpc}$  ( $2\sigma$ ), and  $\delta_g = -0.18 \pm 0.01$  ( $2\sigma$ ) with  $\chi^2_{\text{min}} = 5.97$ . Despite the simplicity of the toy model, the minimum chi-square indicates a good fit, expecting  $\chi^2_{\text{min}} = \nu \pm \sqrt{2\nu}$ . Nevertheless, more complexity is revealed by these counts:  $1.9\sigma$  over-density in bin 3 at  $z \approx 0.09$  hints at the compensation of the supervoid, and bins 4-6 of the  $r = 5^\circ$  counts at redshifts  $0.15 \leq z \leq 0.22$  evidence the deepening of the supervoid in the center, or substructure. For accurate prediction of the effect on the CMB, the density field around the CS region, including any substructure needs to be mapped precisely. This is left for future work, although we present a preliminary tomographic imaging of the region next.

#### 3.3 Tomographic Imaging

For three-dimensional impression of the galaxy distribution around the CS, we created maps in three photo- $z$  slices with a width of  $z < 0.09$ ,  $0.11 < z < 0.14$ , and  $0.17 < z < 0.22$ , and smoothed

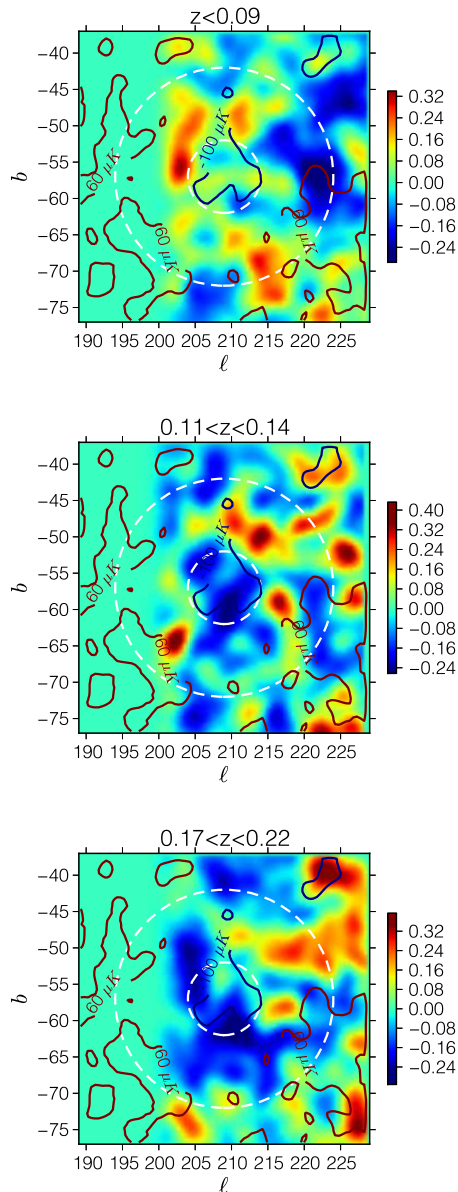


**Figure 4.** Tomographic view of the CS region. The top panel appears to show a foreground over-density at the low redshift. A void is apparent at  $0.11 < z < 0.14$  mostly inside the  $5^\circ$  central region of the CS. The large under-density on the bottom panel at moderately higher redshifts may be slightly off centre with respect to the CS.

with a Gaussian at  $2^\circ$  scales. Then we over-plot the *Planck* SMICA CMB map as contours in Figure 4. The deepest part of the void appears to be close to the centre of the CS in the middle slice.

While photo- $z$  errors do not allow a fine-grained interpretation of the results, we observe a complex structure of voids, possibly a deeper, smaller void nested in a larger, shallower supervoid, or the deepening of a supervoid profile towards the middle. The foreground over density apparent in the first picture, especially the “filament” on the left side running along the PS1 survey boundary further complicates the picture. It is likely to be foreground, since it is more significant in the shallowest slice, gradually fading out at higher  $z$ . These tomographic maps show a compensated surrounding overdense shell around the supervoid at  $r \gtrsim 15^\circ$ , which

plausibly would have fragmented into galaxy clusters visible in the projected slices as several “hot spots” surrounding the CS region. Note that Gurzadyan et al. (2014) uses K-map statistics to *Planck* to show that the CS has a morphological structure similar to a void.

## DISCUSSION & CONCLUSIONS

Using our WISE-2MASS-PS1 data set, we detected a low density region, or supervoid, centred on the CS region: at  $5^\circ$  and  $15^\circ$  radii our detection significances are  $5\sigma$  and  $6\sigma$ , respectively. We measured the galaxy density as a function of redshift at the two predetermined radii. The galaxy underdensity is centred at  $z \simeq 0.22$  for  $15^\circ$ , and even deeper around  $z \simeq 0.15$  for  $5^\circ$ . The counts are consistent with a supervoid of size  $R_{\text{void}} \simeq 192h^{-1}\text{Mpc}$  and average density  $\delta_g \simeq -0.18$ . It is noteworthy that his result is comparable to the local  $300h^{-1}\text{Mpc}$  size underdensity claimed by Keenan et al. (2012) with  $\delta_g \simeq -0.3$ .

To estimate the true underdensity of the supervoid, we modelled the angular power spectrum of the WISE-2MASS galaxy density map using the `python CosmoPy` package<sup>1</sup>, and performed a measurement using `SpICE` (Szapudi et al. 2001). We assume the concordance flat  $\Lambda\text{CDM}$  cosmological model with the amplitude of fluctuations  $\sigma_8 = 0.8$ . We carry out a  $\chi^2$ -based maximum likelihood parameter estimation, finding  $b_g = 1.41 \pm 0.07$ . The minimum value of  $\chi^2_{\text{min}} = 4.72$  is an excellent fit for  $\nu = 7$  degrees-of-freedom that we use in our fit procedure. Note that the value of  $b_g$  contains additional uncertainty due to that of  $\sigma_8$ . This bias is comparable to earlier findings that measured the value of  $b_g$  for 2MASS selected galaxies (Rassat et al. 2007).

The resulting underdensity in the dark matter field, therefore, is  $\delta = \delta_g/b_g \simeq -0.13 \pm 0.03$  assuming a linear bias relation. Given the uncertainties of our toy model, we estimate that the supervoid we detected corresponds to a rare, at least  $3.5\sigma$ , fluctuation in  $\Lambda\text{CDM}$ . The chance alignment of two rare objects is not plausible, therefore a causal relation between the CS and the supervoid is likely.

Using Rudnick et al. (2007), we estimate that the linear ISW effect of this supervoid is of order  $-20 \mu\text{K}$  on the CMB. The effect might be a factor or few higher if the size of the void is larger, if the compensation is taken into account (Pápai et al. 2011), and/or if non-linear and general relativistic effects are included (e.g., Inoue & Silk 2006, 2007). In particular, Finelli et al. (2014) concluded that a non-linear LTB model (Garcia-Bellido & Haugbølle 2008) based on the projected profile in the 2MASS-WISE catalog matches well the profile observed on the CMB.

Superstructures affect several cosmological observables, such as CMB power spectrum and two and three point correlation functions (Masina & Notari 2009b, 2010), CMB lensing (Masina & Notari 2009a; Das & Spergel 2009), 21-cm lensing (Kovetz & Kamionkowski 2013), CMB polarization (Vielva et al. 2011), or cosmic radio dipole (Rubart et al. 2014), and even B-mode polarization (BICEP2 Collaboration 2014). Furthermore, the other CMB anomalies associated with large-angle correlations (Land & Magueijo 2005; Copi et al. 2006, 2013) should be revisited in light of these findings.

Our results suggest the connection between the supervoid and the CS, but further studies addressing the rarity of the observed supervoid observationally would be needed to firmly es-

<sup>1</sup> <http://www.ifa.hawaii.edu/cosmopy/>

establish it. This needs a larger photometric redshift data set that will reach beyond  $50^\circ$  radius, such as PS1 with the second re-processing thus improved calibration, and Dark Energy Survey (The Dark Energy Survey Collaboration 2005). As a first step, we smoothed the projected 2MASS-WISE map with a  $25^\circ$  Gaussian finding only one void as significant as the one we discovered in the CS region. This second void, to be followed up in future research, is clearly visible in the shallow 2MASS maps of Rassat et al. (2013); Francis & Peacock (2010) as a large underdensity, and in the corresponding reconstructed ISW map of Rassat & Starck (2013) as a cold imprint. Therefore we conclude that it is likely to be closer thus smaller in physical size. More accurate photometric redshifts, possibly with novel methods such as that of Ménard et al. (2013), will help us to constrain further the morphology and the size of the void, and a deeper data set would constrain the size of the void in redshift space. Any tension with  $\Lambda$ CDM, e.g. in the possible rarity of the observed supervoid, could be addressed in models of modified gravity, ordinarily screened in clusters, but resulting in an enhanced growth rate of voids as well as an additional contribution to the ISW signal.

## ACKNOWLEDGMENTS

IS acknowledges NASA grants NNX12AF83G and NNX10AD53G. AK and ZF acknowledge support from OTKA through grant no. 101666, and AK acknowledges support from the Campus Hungary fellowship program. BRG acknowledges support from the European Research Council Darklight ERC Advanced Research Grant (# 291521). We used HEALPix (Gorski et al. 2005). The Pan-STARRS1 Surveys (PS1) have been made possible through contributions by the Institute for Astronomy, the University of Hawaii, the Pan-STARRS Project Office, the Max-Planck Society and its participating institutes, the Max Planck Institute for Astronomy, Heidelberg and the Max Planck Institute for Extraterrestrial Physics, Garching, The Johns Hopkins University, Durham University, the University of Edinburgh, the Queen's University Belfast, the Harvard-Smithsonian Center for Astrophysics, the Las Cumbres Observatory Global Telescope Network Incorporated, the National Central University of Taiwan, the Space Telescope Science Institute, and the National Aeronautics and Space Administration under Grant No. NNX08AR22G issued through the Planetary Science Division of the NASA Science Mission Directorate, the National Science Foundation Grant No. AST-1238877, the University of Maryland, and the Eotvos Lorand University (ELTE).

## REFERENCES

Bennett C. L., Larson D., Weiland J. L. e. a., 2012, ArXiv e-prints  
 BICEP2 Collaboration 2014, ArXiv e-prints  
 Bremer M. N., Silk J., Davies L. J. M., Lehnert M. D., 2010, MNRAS, 404, L69  
 Cai Y.-C., Neyrinck M. C., Szapudi I., Cole S., Frenk C. S., 2013, ArXiv e-prints  
 Copi C. J., Huterer D., Schwarz D. J., Starkman G. D., 2006, MNRAS, 367, 79  
 Copi C. J., Huterer D., Schwarz D. J., Starkman G. D., 2013, ArXiv e-prints  
 Cruz M., Martínez-González E., Vielva P., Cayón L., 2005, MNRAS, 356, 29

Cruz M., Martínez-González E., Vielva P., Diego J. M., Hobson M., Turok N., 2008, MNRAS, 390, 913  
 Das S., Spergel D. N., 2009, Phys. Rev. D, 79, 043007  
 Driver S. P., Hill D. T., et al. 2011, MNRAS, 413, 971  
 Finelli F., Garcia-Bellido J., Kovács A., Paci F., Szapudi I., 2014, in prep.  
 Francis C. L., Peacock J. A., 2010, MNRAS, 406, 14  
 Garcia-Bellido J., Haugbølle T., 2008, JCAP, 4, 3  
 Gorski K. M., Hivon E., et al. 2005, ApJ, 622, 759  
 Granett B. R., Neyrinck M. C., Szapudi I., 2008, ApJ, 683, L99  
 Granett B. R., Neyrinck M. C., Szapudi I., 2009, ApJ, 701, 414  
 Granett B. R., Szapudi I., Neyrinck M. C., 2010, ApJ, 714, 825  
 Gurzadyan V. G., Kashin A. L., Khachatryan H., Poghosian E., Sargsyan S., Yegorian G., 2014, ArXiv e-prints  
 Hambly N. C., MacGillivray H. T., Read M. A., et al. 2001, MNRAS, 326, 1279  
 Inoue K. T., Sakai N., Tomita K., 2010, ApJ, 724, 12  
 Inoue K. T., Silk J., 2006, ApJ, 648, 23  
 Inoue K. T., Silk J., 2007, ApJ, 664, 650  
 Kaiser N., 2004, in Society of Photo-Optical Instrumentation Engineers (SPIE) Conference Series  
 Keenan R. C., Barger A. J., Cowie L. L., Wang W.-H., Wold I., Trouille L., 2012, ApJ, 754, 131  
 Kovács A., Szapudi I., 2014, ArXiv e-prints  
 Kovetz E. D., Kamionkowski M., 2013, Physical Review Letters, 110, 171301  
 Kron R. G., 1980, ApJS, 43, 305  
 Land K., Magueijo J., 2005, Physical Review Letters, 95, 071301  
 Masina I., Notari A., 2009a, JCAP, 7, 35  
 Masina I., Notari A., 2009b, JCAP, 2, 19  
 Masina I., Notari A., 2010, JCAP, 9, 28  
 Ménard B., Scranton R., Schmidt S., et al. 2013, ArXiv e-prints  
 Pápai P., Szapudi I., 2010, ApJ, 725, 2078  
 Pápai P., Szapudi I., Granett B. R., 2011, ApJ, 732, 27  
 Pedregosa F., Varoquaux G., Gramfort A., et al. 2011, Journal of Machine Learning Research, 12, 2825  
 Planck 2013 results. XXIII. 2013, ArXiv e-prints  
 Planck 2013 results. XXIV. 2013, ArXiv e-prints  
 Rassat A., Land K., et al. 2007, MNRAS, 377, 1085  
 Rassat A., Starck J.-L., 2013, A&A, 557, L1  
 Rassat A., Starck J.-L., Dupé F.-X., 2013, A&A, 557, A32  
 Rees M. J., Sciama D. W., 1968, Nature, 217, 511  
 Rubart M., Bacon D., Schwarz D. J., 2014, ArXiv e-prints  
 Rudnick L., Brown S., Williams L. R., 2007, ApJ, 671, 40  
 Sachs R. K., Wolfe A. M., 1967, ApJL, 147, 73  
 Schlegel D. J., Finkbeiner D. P., Davis M., 1998, ApJ, 500, 525  
 Skrutskie M. F., Cutri R. M., Stiening R., et al. 2006, AJ, 131, 1163  
 Smith K. M., Huterer D., 2010, MNRAS, 403, 2  
 Szapudi I., Prunet S., Colombi S., 2001, ApJ, 561, L11  
 The Dark Energy Survey Collaboration 2005, ArXiv Astrophysics e-prints  
 Vielva P., 2010, Advances in Astronomy, 2010  
 Vielva P., Martí Nez-González E., Cruz M., Barreiro R. B., Tucci M., 2011, MNRAS, 410, 33  
 Vielva P., Martínez-González E., Barreiro R. B., Sanz J. L., Cayón L., 2004, ApJ, 609, 22  
 Wright E. L., Eisenhardt P. R. M., Mainzer A. K., et al. 2010, AJ, 140, 1868  
 Yan L., Donoso E., Tsai C.-W., et al. 2012, ArXiv e-prints  
 Zhang R., Huterer D., 2010, Astroparticle Physics, 33, 69